ASSOCIATION OF MORB AND SSZ OPHIOLITES ALONG THE SHEAR ZONE BETWEEN COLOURED MELANGE AND BAJGAN COMPLEXES (NORTH MAKRAN, IRAN): EVIDENCE FROM THE SORKHBAND AREA

Morteza Delavari*, Asghar Dolati*, Michele Marroni,°, Luca Pandolfi**,°** and **Emilio Saccani***,✉**

* *Faculty of Earth Sciences, Kharazmi University, Tehran, Iran.*
** *Dipartimento di Scienze della Terra, Università di Pisa, Italy.*
*** *Dipartimento di Fisica e Scienze della Terra, Università di Ferrara, Italy.*
° *Istituto di Geoscienze e Georisorse, CNR, Pisa, Italy.*
✉ *Corresponding author: email: sac@unife.it*

Keywords: *ophiolite, gabbro, harzburgite, geochemistry. Sorkhband, Makran, Iran.*

ABSTRACT

One of the largest worldwide accretionary wedges is exposed in the Makran region (SE Iran). The backstop of this accretionary wedge consists of an imbricate stack of continental and oceanic units, referred as North Makran domain. This domain is characterized by a km-thick shear zone, along which the metamorphic Bajgan Complex is thrust onto the Coloured Mélange Complex. Along this shear zone two slices of ophiolites have been identified in the Sorkhband area. The upper tectonic slice consists of gabbros, whereas the lower one consists of mantle peridotites associated with dunites and chromitite ore deposits. Petrography and geochemistry of gabbros clearly indicate an N-MORB-type affinity, suggesting that they were generated at mid-ocean ridge setting. In contrast, mantle peridotites consist of harzburgites and depleted harzburgites, both showing geochemical features suggesting their genesis in a SSZ setting. The new data presented in this paper indicate that the slices of ophiolites from Sorkhband area derived from two different oceanic domains representing two different geodynamic settings. This occurrence provides new evidence that the boundary between the Coloured Mélange and the Bajgan Complexes represents a first-order tectonic structure that played an important role in the geodynamic evolution of the Makran area.

INTRODUCTION

In the Makran region, SE Iran (Fig. 1), one of the largest worldwide accretionary wedge, is exposed (McCall and Kidd, 1982; Bayer et al., 2006; Burg et al., 2013). This east-west trending accretionary wedge resulted since Eocene from the northward subduction of the oceanic lithosphere of the Oman Sea beneath the Lut and Afghan continental blocks (McQuarrie et al., 2003; Bayer et al., 2006; Vigny et al., 2006; Masson et al., 2007). This accretionary wedge extends between the Minab dextral transform fault to the west, and the sinistral Chaman transform fault to the east, with a width of 300-350 km, more than half exposed onland (McCall and Kidd, 1982; Dercourt et al., 1986; Burg et al., 2008; 2013). The active, submarine frontal part is located southward in the Oman Sea where the ongoing subduction of the oceanic lithosphere shows a rate of about 2 cm/a in a roughly south-to-north direction (McQuarrie et al., 2003; Bayer et al., 2006; Vigny et al., 2006; Masson et al., 2007).

The accretionary wedge has been divided by Burg et al. (2013) into three, main tectono-stratigraphic domains (Fig. 2a) reported as Inner, Outer and Coastal Makran, each representing different segments. The boundaries of these segments are represented by north-dipping, high-angle thrusts whose ages become younger southward (Burg et al., 2013). Northward, these domains are bounded by the North Makran domain that can be regarded as the backstop of the accretionary wedge. The North Makran is represented by an imbricate stack of continental and oceanic units (McCall, 1985; 2002), bounded northward by the Jaz Murian depression (Fig. 2b), considered as a back-arc basin opened at the southern rim of the Lut block as a consequence of the Makran subduction (McCall and Kidd, 1982; McCall, 1985; 1997; Glennie, 2000; Burg et al., 2008; 2013).

The North Makran consists of several tectonic units, described in the literature as geotectonic provinces, each bounded by high-angle shear zones (McCall and Kidd, 1982; McCall, 1985). Some of these units consist of weakly deformed ophiolites, known as Band-e-Zeyarat/Dar Anar (Ghazi et al., 2004), Sorkhband/Rudan (McCall, 2002), Ganj (Shaker-Ardakani et al., 2009), Remeshk-Mokhtarabad (Moslempour et al., 2015), Fannuj-Maskutan (Desmons and Beccaluva, 1983; Moslempour et al., 2015) (Fig. 2a).

Some of these ophiolites, as those from Sorkhband area, occur along the main shear zone that has been found at the base of the Bajgan Complex, that is a metamorphic complex cropping out in the North Makran. The features of these ophiolites, like age, geochemistry and tectonic setting, are fundamental in order to reconstruct the pre-Eocene geodynamic history of the Makran area. However, despite their importance, these ophiolites are still poorly known.

In this paper the geology, petrography and geochemistry of the ophiolites of the Sorkhband area are presented, in order to provide useful elements for the reconstruction of the geodynamic history of the North Makran area.

GEOLOGICAL SETTING OF THE SORKHBAND AREA

The Sorkhband area belongs to the North Makran domain. This domain is characterized by a km-thick shear zone, along which the metamorphic Bajgan Complex is thrust onto the Coloured Mélange Complex (Fig. 3). This is one of the most important shear zones of the North Makran that can be recognized as a several km-thick, highly deformed assemblage of slices with variable sizes. Although most of the slices show a thickness ranging from 1 to 10 meters, some of them consist of coherent bodies whose thicknesses attain almost 4-5 km.

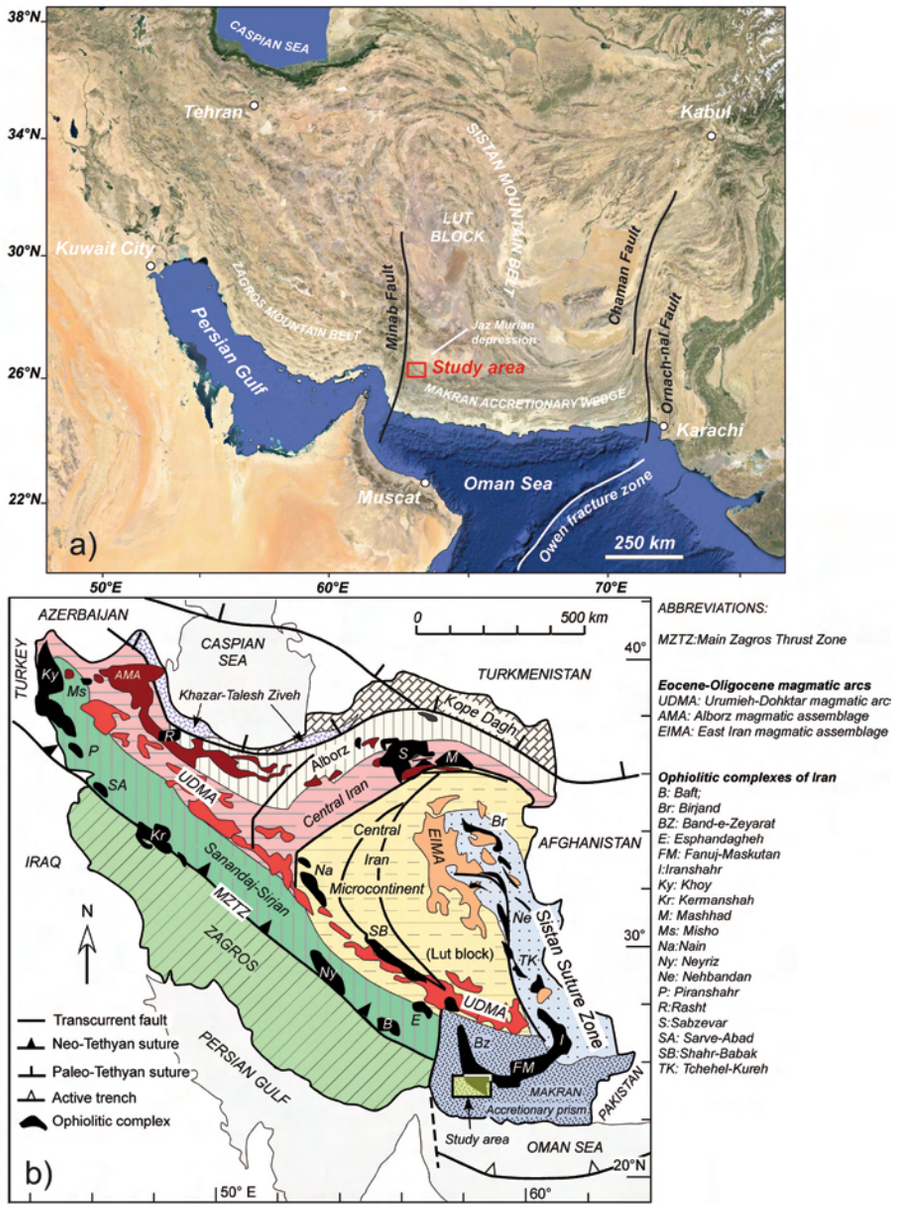

Fig. 1 - Geographic and geological location of the Sorkhband ophiolites: Satellite image (a) and geological sketch map (b) of Iran. The main ophiolite massifs of Iran are shown (modified after Grando and McClay, 2007; Saccani et al., 2013). In both the figures the study area is boxed.

This shear zone occurs at the base of the Bajgan Complex, a metamorphic assemblage of schists, paragneisses, amphibolites and marbles. Metamorphism ranges from greenschist to amphibolite facies, but scattered occurrences of glaucophane is reported (McCall, 2002). Devonian fossils are reported in the Bajgan Complex by McCall (1985). The age of the metamorphism is unknown, but the occurrence of undeformed Jurassic deposits that lies unconformably over the Bajgan Complex (McCall, 2002) suggests a Paleozoic age or older. In addition, the scattered occurrence of serpentinites with uncertain tectonic position is also reported (McCall, 2002). To the east, the Bajgan Complex shows a transition to the Durkan Complex of the North Makran, which consists of a ~ 250 km-long and ~ 40 km-wide slice of continental crust (McCall, 1985) made up of an assemblage of Jurassic plutonic bodies associated with Cretaceous lava, as well as shallow and deep marine, Permian to Cretaceous, sedimentary rocks (Hunziker et al., 2015, and quoted references). To the west, the Bajgan Complex continues in the Sanandaj-Sirjan zone, i.e. a ~ 1500 km-long metamorphic belt that extends from the northwest (Sanandaj) to southeast (Sirjan), parallel to the Zagros Fold and Thrust belt (Ghazi and Moazzen, 2015 and quoted references).

The Bajgan Complex overlies a tectonic mélange referred by Gansser (1955; 1959) and McCall (1983) as Coloured Mélange Complex that also crops out immediately below the Durkan Complex. This mélange consists of an assemblage of m-thick slices without any evidence of sedimentary and/or tectonic matrix. The slices consist of serpentinites, gabbros, basalts, cherts, shales and limestones. Slices of Globigerinids-bearing limestones of Early Paleocene age and metamorphic rocks, such as schists and amphibolites, have been found as well.

The Coloured Mélange Complex is, in turn, thrust onto the tectonic units of the Inner Makran (Fig. 2) consisting of Late Eocene to Early Miocene siliciclastic turbidites conformably topped by Paleocene to Middle Eocene pelagic sediments and volcanic rocks (Burg et al., 2013). The boundary between North and Inner Makran is represented by the Bashakerd thrust, a main fault zone separating two geologically different domains.

The relationships between the Coloured Mélange and

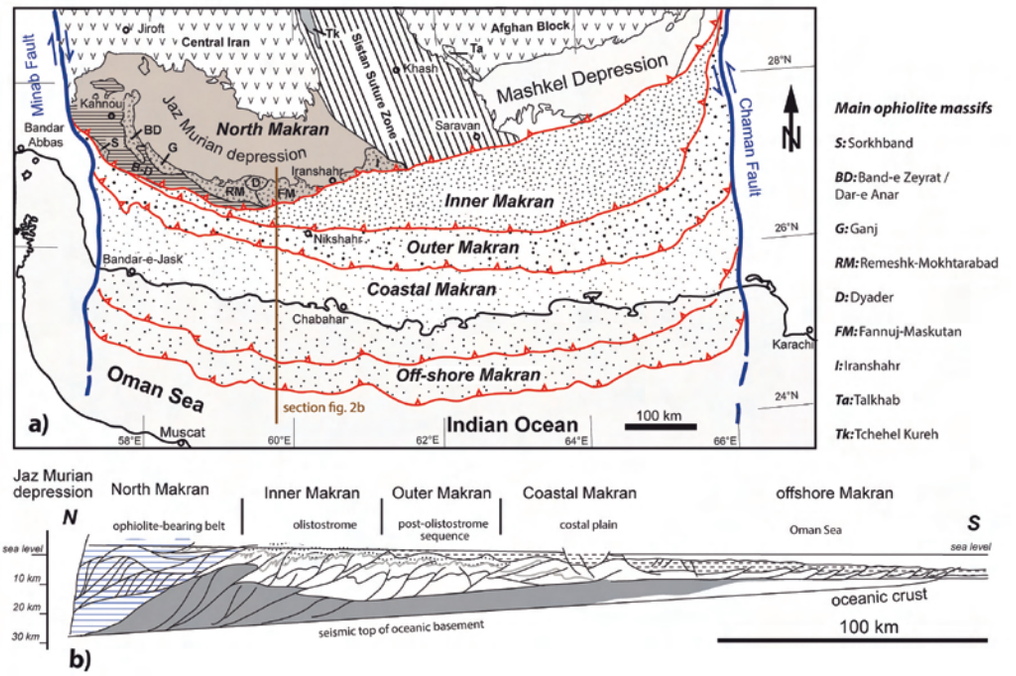

Fig. 2 - Tectonic sketch map of the Makran region (a) and related cross section (b). The location of the ophiolites belonging to the North Makran is shown. Modified after Dolati and Burg (2013).

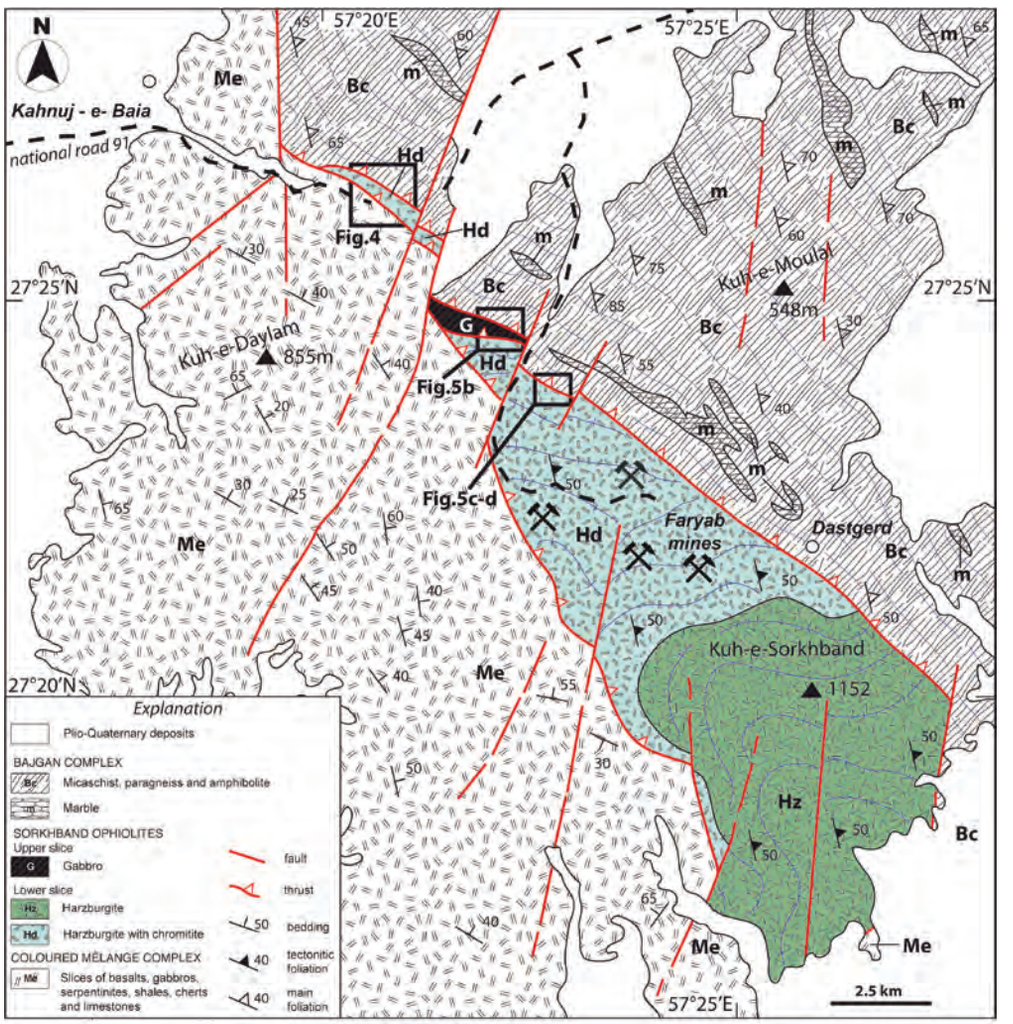

Fig. 3 - Geological map of the Sorkhband ophiolites (modified after Morgan et al., 1979). The location of Figs. 4 and 5 is indicated.

the Bajgan Complex can be observed along the road 91 from Bandar Abbas to Kahnuj (Fig. 4), just 17 km west of city of Manujan in correspondence of the tunnel. The strike of the contact is NW-SE with an east dipping of 25-30° (Fig. 4a). The sense of shear is top-to-the W. In this area, a slice of serpentinized harzburgites bounded by two shear zones occurs between the Coloured Mélange and the Bajgan Complexes (Fig. 4b). These shear zones are both represented by an about 100 m-thick higly deformed bands where m-thick elongated and boudinaged bodies of marbles, metabasalts and serpentinized peridotites are imbricated (Fig. 4c).

In the Sorkhband area (Fig. 3), the shear zone at the base of Bajgan Complex is characterized by the occurrence of two different slices of ophiolites. The uppermost one consists of coarse-grained gabbros cut by dykes of fine-grained gabbros. This slice is about 200 m-thick. The gabbro slice is thrust onto a huge slice of oceanic mantle-lower crust transition zone (Behzadi and Shahabpour, 2011; Najafzadeh, 2012; Jannessary et al., 2012; Rajabzadeh and Moosavinasab, 2013), whose thickness attains 3-4 km. The tectonic relationships between the upper slice of Sorkhband ophiolites and the Bajgan Complex are well exposed south of the buildings of the chromium mine of Faryab-Shahin

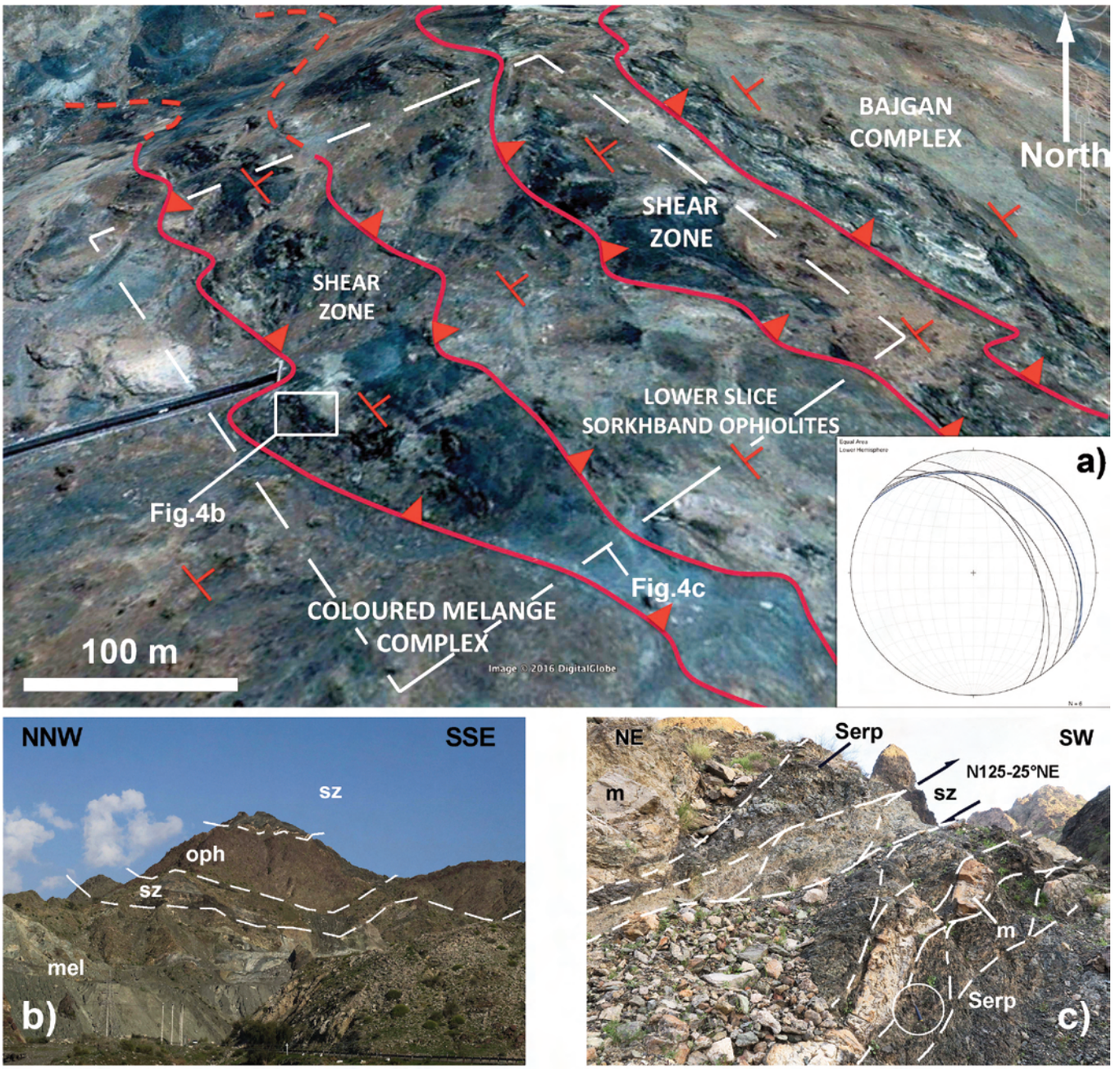

Fig. 4 - Relationships among the Coloured Mélange Complex, the Sorkhband ophiolites and the Bajgan Complex in correspondence of the tunnel along the road 91, 17 km west of Manujan (modified from Google Earth image). The tectonic surfaces and its attitude as well as the bedding in the Coloured Mélange are shown. a) Stereographic projection of the shear zone surfaces (Schmidt net, lower hemisphere). b) and c) Details of the field relationships between the Coloured Mélange unit and the shear zone (sz- shear zone; oph- lower slice of Sorkhband Ophiolites; mel- Coloured Mèlange; m- metalimestones; Serp- serpentinite slices). The location of the field pictures are indicated also in Fig. 3.

(Fig. 5). The strike of the contact is NW-SE with an east dipping of 50-60° (Fig. 5a). The sense of shear is top-to-the SW. The contact zone between the slice of gabbros and the Bajgan Complex consists of a 60 m-thick shear zone associated with a 30-m thick slice of metabasalts (Fig. 5b). The shear zone consists of m-thick elongated bodies of serpentinites, paragneisses, marbles and metabasalts. Southwards, the slice of gabbros is boudinaged along the shear zone and the Bajgan Complex directly overlies the peridotites of the lower slice of the Sorkhband ophiolites (Fig. 5c). Also in this area, the boundary between the slice of peridotites and the Bajgan Complex is characterized by a 30 m-thick shear zone where m-thick elongated and boudinaged bodies of serpentinites and metamorphic rocks, mainly metabasalts, are imbricated (Fig. 5d).

OPHIOLITES OF THE SORKHBAND AREA

Ophiolites in the Sorkhband area are located 7 km southwest of the city of Manujan. They crop out on about 50 km^2 along a NW-SE belt (Fig. 2), where is located the chromium mine of Faryab. The tectonic setting of these ophiolites consists of two different tectonic slices; the upper one consists

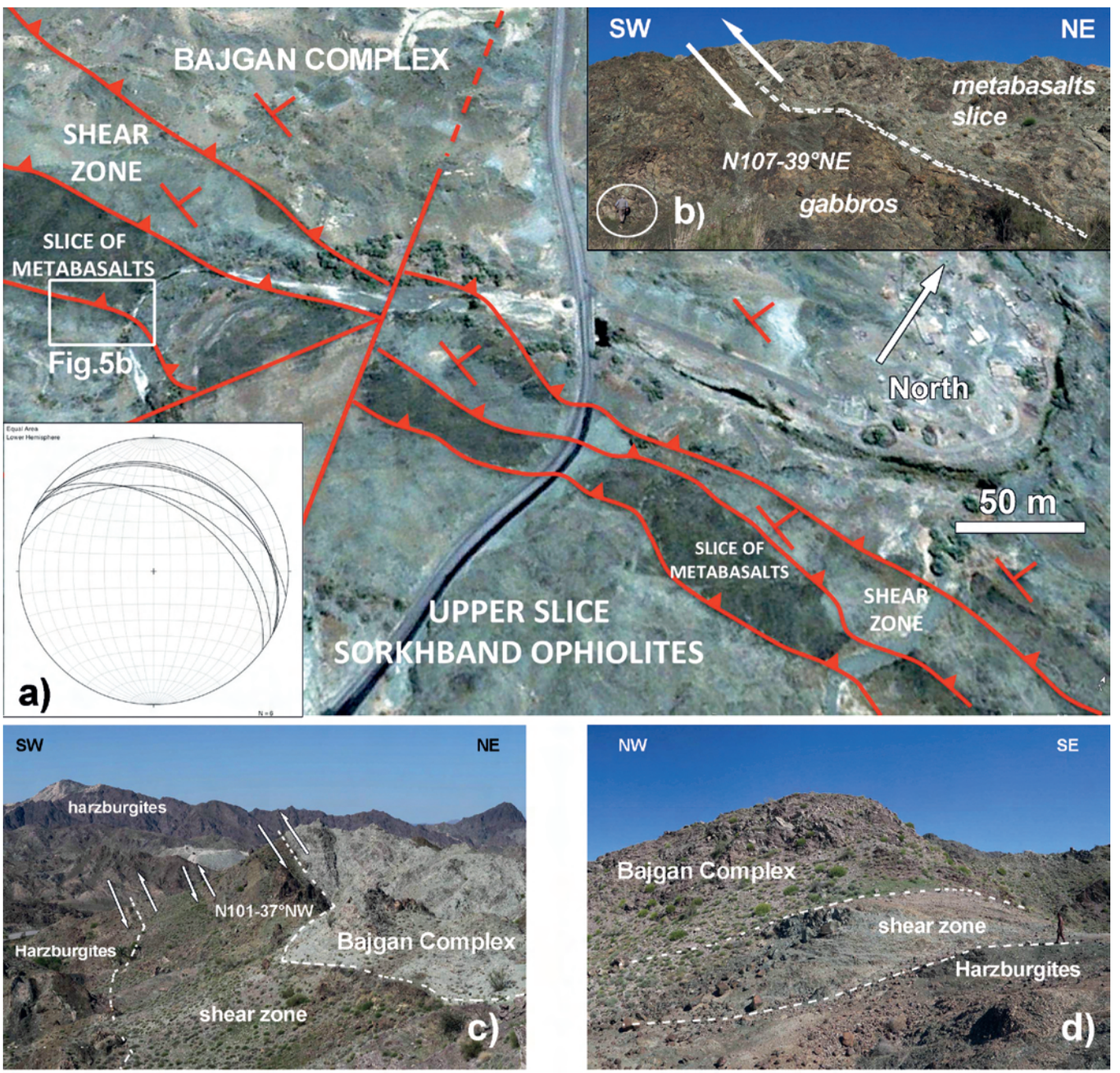

Fig. 5 - Relationships among the the Sorkhband ophiolites and the Bajgan Complex in correspondence of the Faryab-Shahin mines, 6 km south of the mining company main building (modified from Google Earth image). The tectonic surfaces and its attitude, as well as the main foliation in the Bajgan Complex are shown. a) Stereographic projection of the shear zone surfaces (Schmidt net, lower hemisphere). b) thrusting of the metabasalts (Bajgan Complex) onto the gabbros belonging to the upper slice of the Sorkhband ophiolites. c) and d) field relationships between the lower slice of the Sorkhband ophiolites and the Bajgan Complex. The location of the field pictures are indicated also in Fig. 3.

of gabbros, whereas the lower one is mainly represented by mantle peridotites. Both these tectonic slices have been sampled in order to define their petrographic and geochemical features, as well as their tectono-magmatic significance.

Analytical methods

Whole-rock major and the trace elements Zn, Cu, Sc, Ga, Ni, Co, Cr, V, and Ba were analyzed by X-ray fluorescence (XRF) on pressed-powder pellets, using an ARL Advant-XP automated X-ray spectrometer. The matrix correction method proposed by Lachance and Trail (1966) was applied. Volatile contents were determined as loss on ignition (L.O.I.) at 1000°C. CO_2 content was determined by simple volumetric technique (Jackson, 1958). This technique was calibrated using standard amounts of reagent grade $CaCO_3$. In addition, Rb, Sr, Y, Zr, Nb, Hf, Ta, Th, U, and rare earth elements (REE) were determined by inductively coupled plasma-mass spectrometry (ICP-MS) using a Thermo Series X-I spectrometer. All analyses were performed at the Dipartimento di Fisica e Science della Terra, Università di Ferrara.

Accuracy and detection limits for both XRF and ICP-MS analyses were determined using several international reference materials, as well as internal standards run as unknowns. Accuracy and detection limits for CO_2 measurement were estimated by analyzing different amounts of reagent grade $CaCO_3$. Accuracy and detection limits are reported in Table 1 together with whole-rock compositions.

Upper ophiolite tectonic slice

Stratigraphy

This slice consists of 200 m-thick coarse-grained gabbros (Fig. 6a) cut by m-thick dykes of fine-grained gabbros. Most of the gabbros are cataclastic, but well-preserved bodies where the magmatic textures can be still observed are also recognized. The age of these ophiolites is unknown.

Petrography

The gabbros (MK75, MK76, MK78) are very altered. Nonetheless, the original texture and rock-forming minerals can still be recognized. They are coarse-grained and consist of plagioclase, clinopyroxene, and oxide minerals. All samples show isotropic texture with euhedral plagioclase and subhedral clinopyroxene. Plagioclase is totally transformed either to sericite or clay minerals, but the original twinning can locally be recognized. Clinopyroxene is completely altered to chlorite or amphibole. In sample MK75, rounded or lobate opaque minerals show altered rims. In sample MK76 plagioclase show deformed twinning. Sample MK78 contains significant amount of granular epidote and secondary amphibole locally showing a vague foliation. Small veins

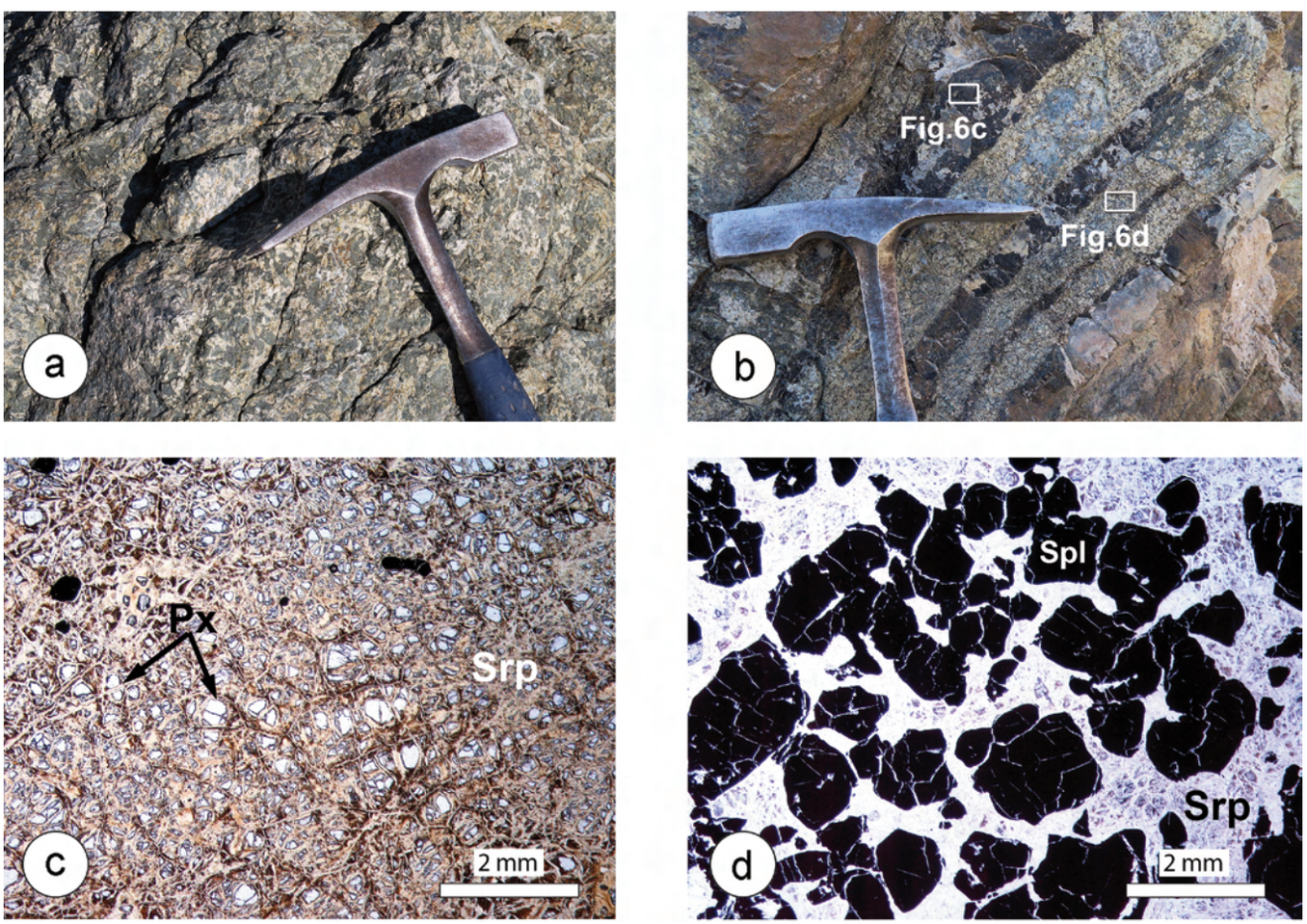

Fig. 6 - Field and microscopic features of the Sorkhband ophiolites. a) gabbros of the upper slice of the Sorkhband ophiolites; b) bands of chromite-rich layers in harzburgites in the lower slice of the Sorkhband ophiolites; c) photomicrograph of the harzburgites (Px- pyroxene; Srp- serpentine); d) photomicrograph of the chromite-rich layers (Spl- Cr-spinel; Srp- serpentine minerals). The location of Fig. 6c and d is indicated in Fig. 6b.

Table 1 - Bulk-rock major and trace element analyses of samples from the upper and lower ophiolite tectonic slices in the Sorkhband area.

	Upper tectonic slice (gabbros)			Lower tectonic slice (peridotites)				Analytical details	
Sample	MK76	MK78	MK75	MK82	MK85	MK83	MK84	Accuracy	Detection limits
Rock Type	gabbro N-MORB	gabbro N-MORB	gabbro N-MORB dyke in gabbro	harzb	harzb	D-harzb	D-harzb		
Note								(absolute relative error %)	
XRF analyses:								BE-N	
(wt%)									
SiO_2	52.43	57.03	56.27	38.97	38.07	42.41	35.19	0.3	0.05
TiO_2	0.49	0.41	0.63	0.03	0.02	0.02	0.01	0.3	0.01
Al_2O_3	12.97	11.46	11.95	1.83	1.04	1.39	0.92	3.4	0.05
Fe_2O_3	0.82	0.39	0.67					1.3	0.10
FeO	5.48	2.59	4.47	5.61	4.41	7.06	8.72		
MnO	0.13	0.08	0.13	0.11	0.10	0.11	0.14	7.4	0.05
MgO	8.23	7.00	7.32	38.93	37.59	43.66	42.27	2.8	0.01
CaO	12.93	13.23	11.82	0.81	2.97	1.18	0.04	1.9	0.04
Na_2O	2.97	6.17	5.25	n.d.	n.d.	n.d.	n.d.	2.7	0.01
K_2O	0.04	0.02	0.03	n.d.	n.d.	0.01	n.d.	3.6	0.01
P_2O_5	0.07	0.02	0.07	n.d.	n.d.	n.d.	n.d.	6.4	0.01
LOI	3.48	1.64	1.47	13.72	14.01	4.12	12.78		
CO_2	n.d.	n.d.	n.d.	n.d.	1.76	n.d.	n.d.	1.4	0.22
Total	100.04	100.05	100.08	100.02	99.97	99.95	100.07		
Mg#	72.8	82.8	74.5	92.5	93.8	91.7	89.6		
(ppm)									
Zn	n.d.	n.d.	n.d.	4	n.d.	n.d.	n.d.	3.3	2
Cu	7	n.d.	28	17	n.d.	6	3	0.8	3
Sc	37	34	44	17	36	10	6	4.6	3
Ga	25	13	15	n.d.	n.d.	n.d.	n.d.	4.4	3
Ni	34	26	29	2231	790	2142	1637	2.2	2
Co	36	29	36	126	103	125	153	5	2
Cr	63	138	138	3085	3772	2751	3201	2.2	2
V	190	272	285	63	55	35	19	1.7	2
Ba	24	10	16	n.d.	n.d.	n.d.	n.d.	3.3	3
ICP-MS analyses:								BHVO-1	
(ppm)									
Rb	0.298	0.193	0.364	0.129	0.129	0.379	0.002	1.4	0.02
Sr	74.3	101	152	3.42	2.82	0.857	0.833	1.7	0.02
Y	19.8	11.8	22.2	1.23	0.620	0.270	0.260	2.8	0.003
Zr	32.1	23.3	29.0	0.639	0.261	0.157	0.089	6.1	0.02
La	1.69	0.683	1.49	0.009	0.007	0.050	0.042	1.3	0.01
Ce	5.11	2.15	4.65	0.037	0.035	0.104	0.073	3.7	0.002
Pr	0.934	0.419	0.904	0.011	0.012	0.014	0.009	2.3	0.004
Nd	5.12	2.39	5.21	0.101	0.080	0.048	0.037	3.7	0.002
Sm	1.77	0.959	1.95	0.047	0.036	0.012	0.013	5.3	0.006
Eu	0.754	0.450	0.912	0.020	0.015	0.004	0.005	1.9	0.002
Gd	2.44	1.36	2.81	0.086	0.059	0.017	0.018	2.3	0.001
Tb	0.430	0.248	0.500	0.020	0.012	0.003	0.004	3.6	0.002
Dy	2.97	1.74	3.48	0.163	0.090	0.027	0.024	4.2	0.001
Ho	0.626	0.378	0.730	0.041	0.022	0.008	0.006	6.1	0.002
Er	1.87	1.11	2.16	0.124	0.064	0.026	0.019	7.1	0.001
Tm	0.292	0.172	0.333	0.020	0.010	0.005	0.003	4.5	0.003
Yb	1.95	1.11	2.21	0.150	0.065	0.041	0.022	6.9	0.001
Lu	0.300	0.190	0.339	0.027	0.011	0.008	0.004	6.9	0.004
Nb	1.27	0.855	1.11	0.166	0.239	0.104	0.209	2.7	0.001
Hf	0.854	0.445	0.662	0.025	0.007	0.003	0.002	2.1	0.001
Ta	0.076	0.049	0.059	0.004	0.004	0.012	0.005	5.7	0.005
Th	0.080	0.027	0.043	0.008	0.006	0.013	0.015	4.6	0.0015
U	0.039	0.019	0.025	0.003	0.005	0.005	0.006	7.1	0.002
Nb/Y	0.06	0.07	0.05						
$(La/Sm)_N$	0.62	0.46	0.49	0.12	0.12	2.57	2.06		
$(Sm/Yb)_N$	1.01	0.96	0.98	0.35	0.62	0.34	0.65		
$(La/Yb)_N$	0.62	0.44	0.48	0.04	0.07	0.87	1.35		

Accuracy and detection limits for both X-Ray Fluorescence spectrometry (XRF) and Inductively Coupled Plasma-Mass Spectrometry (ICP-MS) are also reported. Accuracy was estimated using recommended values for international reference materials BE-N and BHVO-1 (Govindaraju, 1994), whereas detection limits were estimated using repeated measures of 29 international reference standards run as unknowns. Abbreviations: harzb- harzburgite; D-harzb- depleted harzburgite; N-MORB- normal-type mid-ocean ridge basalt; n.d.- not detected. Mg# = molar Mg*100/(Mg + Fe); Fe_2O_3 in mafic rocks is assumed as Fe_2O_3 = FeO x 0.15.

filled by secondary quartz are observed in samples MK75 and MK78. All samples show mm-scale deformations. The crystallization order in these rocks is: plagioclase + clinopyroxene ± opaque minerals, that is the typical crystallization order observed in mid-ocean ridge-type gabbros.

Geochemistry

Two of three of the intrusive rocks studied in this paper (MK78, MK75) show rather high silica content (SiO_2 = 56.27-57.03 wt%), which is related to the occurrence of veins of secondary quartz in these samples (see the Petrography section). However, all other elements are in the compositional range for gabbroic rocks. Therefore, we classify all intrusive rocks as gabbros. They show relatively low TiO_2 (0.41-0.63 wt%), P_2O_5 (0.02-0.07 wt%), Y (11.8-22.2 ppm), and Zr (23.3-32.1 ppm) contents with Mg# [defined as Mg*100/(Mg + Fe)] ranging from 72.8 to 82.8. MgO (7.00-8.23 wt%) and Al_2O_3 (11.46-12.97 wt%) contents are relatively low. These rocks are depleted in incompatible elements with respect to N-MORB composition. Nonetheless, they show rather flat N-MORB normalized patterns (Fig. 7a), which are similar to those of MORB-type gabbros. Chondrite-normalized REE patterns (Fig. 7b) show the typical N-MORB trends with flat medium REE (MREE) and heavy REE (HREE) coupled with light REE (LREE) depletion with $(La/Yb)_N$ ratio (normalized to the chondrite composition, Sun and McDonough, 1989) ranging from 0.44 to 0.62. Samples MK75 and MK76 have absolute REE contents ranging from ~ 6 to ~ 13 times chondrite composition, that is, their REE concentrations are only slightly depleted with respect to the N-MORB composition. In contrast, sample MK78 shows depletion in REE content compared to N-MORB, with absolute REE contents ranging from ~ 3 to ~ 8 times chondrite composition (Fig. 7b). All samples display Eu positive anomalies, which is consistent with the earlier crystallization of plagioclase described in the petrography section.

According to Serri (1981), the magmatic affinity of gabbroic rocks can be deduced on the basis of the mutual relationships between TiO_2 contents and FeO/(FeO + MgO) ratios. The diagram in Fig. 8 shows that Sorkhband gabbros plot in the field of high-Ti (i.e., MORB) gabbros. The discrimination diagrams in Fig. 9 (Saccani, 2015) and Fig. 10 (Wood, 1980) should be used with some caution when plotting gabbroic rocks. In fact, in contrast to volcanic rocks, the composition of gabbroic rocks may be influenced by cumulus processes or mineral segregation from their parental liquids. Nonetheless, the isotropic texture of the studied gabbros and their relatively low MgO and Al_2O_3 contents suggest that they were not affected by significant segregation of either plagioclase or pyroxene and therefore their composition can reasonably be assumed as representing liquid composition. Once plotted in these diagrams, the Sorkhband gabbros plot in the fields for N-MORB compositions, further supporting the origin of these rocks in mid-ocean ridge setting.

Lower ophiolite tectonic slice

Stratigraphy

This slice consists of a well exposed thick sequence of mantle peridotites with remnants of lower oceanic crust. At its base the sequence includes layered diopside-bearing harzburgites associated with minor lenticular bodies of dunites (Figs. 6b, c and d). Both harzburgites and dunites are cut by clinopyroxenite dykes. The harzburgites show a gradual transition to a thick level of dunites with minor bands of wherlites and websterites. Also the dunites are cut by dykes of ol-bearing clinopyroxenites. Podiform ore bodies of chromitites have been found in the dunites with different shape and size as pods, lenses, bands and rich dissemination (Najafzadeh et al., 2008), but bands of chromitites have also been observed inside the mantle peridotites. The age of these ophiolites is still unknown, but probably they are Cretaceous in age as suggested by Ghazi et al. (2004), according to the lack of any orogenic metamorphism. However, an Ordovician age for these ophiolites has also been suggested by Najafzadeh et al. (2008).

Petrography

Peridotites MK82, MK84, and MK85 are almost totally serpentinized, whereas sample MK83, though very altered shows some recognizable textural and mineralogical features. Sample MK82, beside serpentine minerals, contains

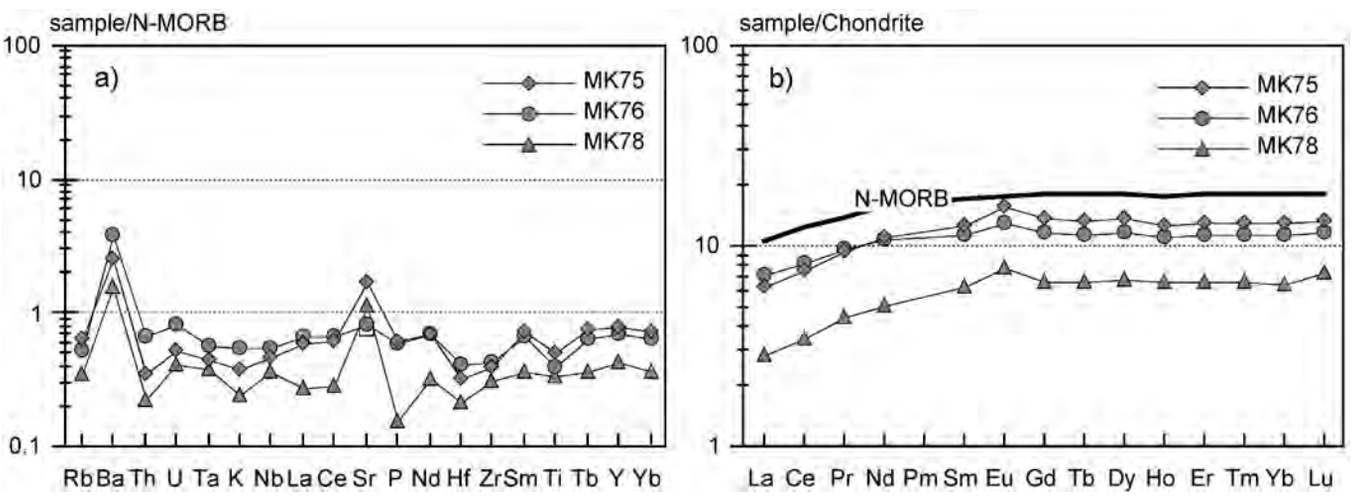

Fig. 7 - N-MORB normalized incompatible element abundance patterns (a) and chondrite-normalized REE abundance patterns (b) for gabbros from the upper ophiolite tectonic slice in the Sorkhband area. The composition of typical mid-ocean ridge basalt (N-MORB) in panel b) and normalizing values are from Sun and McDonough (1989).

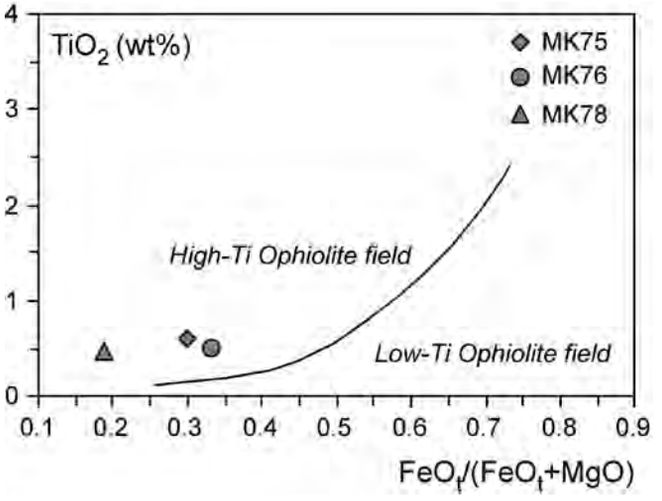

Fig. 8 - TiO_2 vs. $FeO_t/(FeO_t + MgO)$ discrimination diagram for gabbros from the upper ophiolite tectonic slice in the Sorkhband area. Modified from Serri (1981).

small amount of hydroxides and some altered minerals most likely derived from original pyroxene. Sample MK83 shows relics of olivine and orthopyroxene, as well as euhedral chromian-spinel as accessory phase. Orthopyroxene shows large exsolution lamellae of clinopyroxene. Sample MK84 is characterized by very small rounded relics of olivine and abundant, apparently fresh chromian-spinel. Sample MK85 shows banded texture due to the different orientation of serpentine minerals. Bands are about 1 cm wide. Some relics of orthopyroxene with exsolution lamellae can be recognized. Based on the occurrence of orthopyroxene relics, samples MK82, MK83, and MK85 can be classified as harzburgites. In contrast, sample MK84 cannot be reliably classified because of the complete serpentinization.

Geochemistry

As described in the petrography section, peridotitic samples are generally very altered. The only exception is represented by sample MK83, which is moderately altered. The very high LOI values in samples MK82, MK83, MK85 and the relatively low LOI value in sample MK84 further support this observation (Table 1). To verify if serpentinization resulted in major element changes, our samples were plotted in the MgO/SiO_2 vs. Al_2O_3/SiO_2 diagram (Fig. 11). In this diagram, fresh mantle peridotites define the "terrestrial array" (Jagouts et al., 1979; Hart and Zindler, 1986). Fig. 11 shows that, except sample MK84, the studied mantle peridotites plot very close to the "terrestrial array" suggesting that, though very intense, serpentinization produced very limited modifications in terms of SiO_2, Al_2O_3, and MgO contents. In contrast, sample MK84 has MgO content too high compared to its silica concentration. The contents of some selected major and trace elements of peridotites from the Sorkhband area are plotted versus MgO content in Fig. 12. In peridotites, abundances of Al_2O_3, CaO, TiO_2, Sc and V are expected to show well-defined inverse correlations with MgO. In contrast, Ni is expected to show well-defined positive correlation with MgO. Snow and Dick (1995) have shown that seafloor weathering may results in the loss of MgO and Ni and increase of alkali elements and Al_2O_3. However, although the data set is limited, the chemistry of the studied peridotites is somewhat contradictory. The alkali content is very low in all samples (< 0.01 wt%) implying that these peridotites were not affected by significant addition of alkali elements during seafloor weathering. In sample MK82, the Al_2O_3 and Sc contents are too high for its low CaO and TiO_2 contents and high Ni and V values (Fig. 12). Sample MK85 has Al_2O_3, CaO, and TiO_2 contents, which are consistent with relatively low MgO value. Nonetheless, Ni and Sc contents are too low and too high, respectively when compared to MgO content. According to

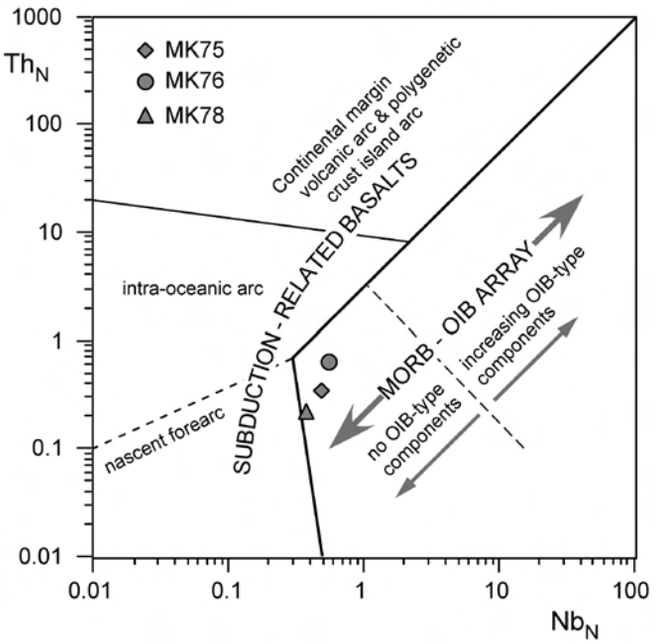

Fig. 9 - N-MORB normalized (Sun and McDonough, 1989) Th vs. Nb discrimination diagram (Saccani, 2015) for the gabbros from the upper ophiolite tectonic slice in the Sorkhband area.

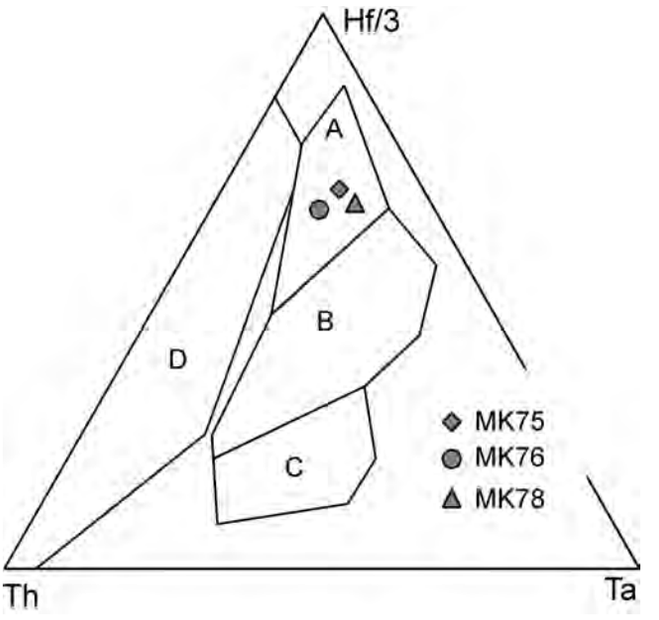

Fig. 10 - Th, Ta, Hf/3 discrimination diagram (Wood, 1980) for the gabbros from the upper ophiolite tectonic slice in the Sorkhband area. Fields: A- normal mid-ocean ridge basalt; B- transitional mid-ocean ridge basalt and within-plate tholeiite; C- within-plate alkali basalt; D- volcanic arc basalt.

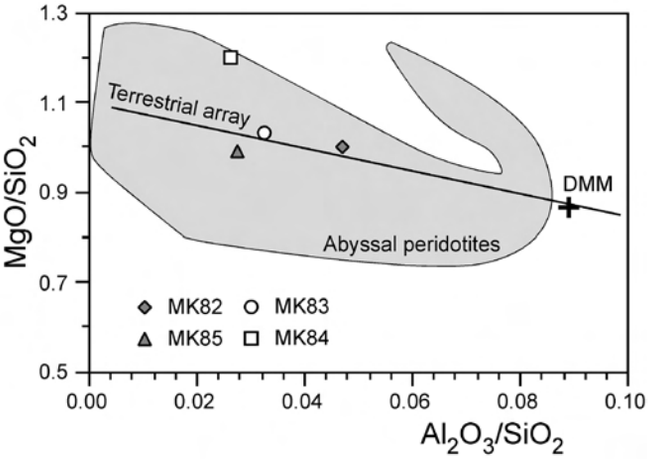

Fig. 11 - Whole rock MgO/SiO_2 vs. Al_2O_3/SiO_2 diagram for Albanide-Hellenide mantle peridotites. Major element concentrations are recalculated to 100% on LOI-free and secondary calcite-free bases. The "terrestrial array" is from Jagoutz et al. (1979) and Hart and Zindler (1986). Abyssal peridotites data from PetDB database (http://www.earthchem.org).

its relatively less altered nature, sample MK83 is the only one in which the concentration of all element is consistent with its MgO content. Sample MK84 show relatively high Al_2O_3 content and relatively low CaO and Ni contents compared to its high MgO content.

Chondrite-normalised REE patterns (Fig. 13) basically show two populations of samples. Samples MK82 and MK85 are characterized by severe depletion in LREE compared to MREE and HREE, with $(La/Sm)_N = 0.12$ and $(La/Yb)_N = 0.04\text{-}0.07$. In contrast, samples MK83 and MK84 show U-shaped chondrite-normalized REE patterns with $(La/Sm)_N = 2.06\text{-}2.57$ and $(La/Yb)_N = 0.87\text{-}1.35$. Moreover, when compared to samples MK82 and MK85, these samples have lower absolute concentrations of HREE and higher absolute concentrations of LREE.

The overall chemical composition of the studied peridotites points out for a depleted nature of these rocks. All samples show significant depletion with respect to the depleted MORB mantle (DMM) composition (Workman and Hart, 2005) (Figs. 12 and 13). REE contents in samples MK82 and MK85 are compatible with the REE composition of clinopyroxene-bearing harzburgites (or, eventually very depleted lherzolites). Unfortunately, the severe alteration of these rocks does not allow clinopyroxene to be recognized in these samples. In contrast, the comparatively low HREE contents coupled with LREE/MREE enrichment observed in samples MK83 and MK84 are compatible with the REE composition of very refractory, depleted harzburgites (Fig. 13). Accordingly, in sample MK83, in which the original mineral assemblage can still be recognized, no clinopyroxene is observed. In summary, the depleted nature of the Sorkhband mantle peridotites indicates that they represent residual mantle formed at supra-subduction zone (SSZ) setting (see the discussion in the next section).

DISCUSSION

The shear zone between the Coloured Mélange Complex and the pair Bajgan and Durkan Complexes is one of the most prominent tectonic elements of the North Makran. This element can be recognized as a NW-SE to E-W striking belt of deformed rocks extending for about 500 km along the whole Makran area up to the Sinadaj-Sirjan zone. This shear zone is pre-Eocene in age, according to the occurrence of the Eocene sedimentary deposits that unconformably seal the relationships between the Coloured Mélange Complex and both the Bajgan and Durkan Complexes (McCall, 1997; 2002, Burg et al., 2013). This shear zone is characterized by slices of ophiolites, not only in the Sorkhband area but also in the Rudan area. In the Sorkhband area, two different ophiolitic tectonic slices have been recognized; the upper one is characterized by gabbros, whereas the lower one consists of mantle peridotite with remnants of its associated lower crust. Some authors have suggested an Ordovician age for these ophiolites (Najafzadeh et al., 2008). However, no clear evidence is provided in support of this conclusion. Based on the absence of any ductile deformation, as well as medium- to high-grade metamorphism, which commonly characterize the Paleozoic units in this area, we favour the hypothesis of a Mesozoic (i.e., Jurassic or Late Cretaceous) age for the ophiolite sequences.

The petrographic and geochemical data indicate that gabbros forming the upper tectonic slice were generated at mid-ocean ridge setting, whereas mantle peridotites of the lower tectonic slice were generated at SSZ setting. Similar associations of SSZ-type mantle peridotites and MOR-type crustal rocks are common in many Mesozoic ophiolitic complex in Iran as, for example, the Late Cretaceous Haji-Abad (Esfandagheh) ophiolites located in the outer ophiolite Zagros belt (Shafaii Moghadam and Stern, 2011; Shafaii Moghadam et al., 2013), the Kermanshah ophiolite located at the northwestern end of the Zagros belt (Ghazi and Hassanipak, 1999; Allahyari et al., 2010; Saccani et al., 2013; Whitechurch et al., 2013), and the Nehbandan ophiolite in the Sistan Suture Zone (Delavari et al., 2009; Saccani et al., 2010). These ophiolites include remnants of Mesozoic oceanic basins, as well as intra-oceanic SSZ settings. Similar to the Sorkhband ophiolites, they consist of mantle tectonites including cpx-poor lherzolites, harzburgites, and depleted harzburgites with widespread dunite lenses with podiform chromitites, as well as crustal sections in which gabbroic rocks are well represented. However, in contrast to the Sorkhband ophiolites, these ophiolites also include mafic-ultramafic cumulates, and both pillow and massive lava flows. Compared to the Sorkhband upper tectonic slice, the geochemistry of crustal rocks of these ophiolites is more complex. In the Kermanshah ophiolite, gabbros show both normal-MORB (N-MORB) and enriched MORB (E-MORB) chemistry, whereas the volcanic sequence includes E-MORB, plume-type MORB (P-MORB) and alkaline within-plate basalts (Allahyari et al., 2010; Saccani et al., 2013). In the Haji-Abad ophiolite, the geochemistry of volcanic rocks show a magmatic progression from E-MORB-type pillow lavas to boninitic lavas, that is a magmatic progression from an oceanic setting to a nascent forearc setting (Shafaii Moghadam et al., 2013). In the Nehbandan ophiolite, two different types of mafic-ultramafic intrusive series can be observed. One is composed of MOR-type rocks, whereas the other is composed of SSZ-type rocks (Saccani et al., 2010). Several authors have suggested that both the Zagros belt and Sistan ophiolites record two different stages of oceanic evolution. The first stage corresponds to oceanic spreading and formation of MORB-type lithosphere commonly influenced by ocean island basalt (OIB) enriched

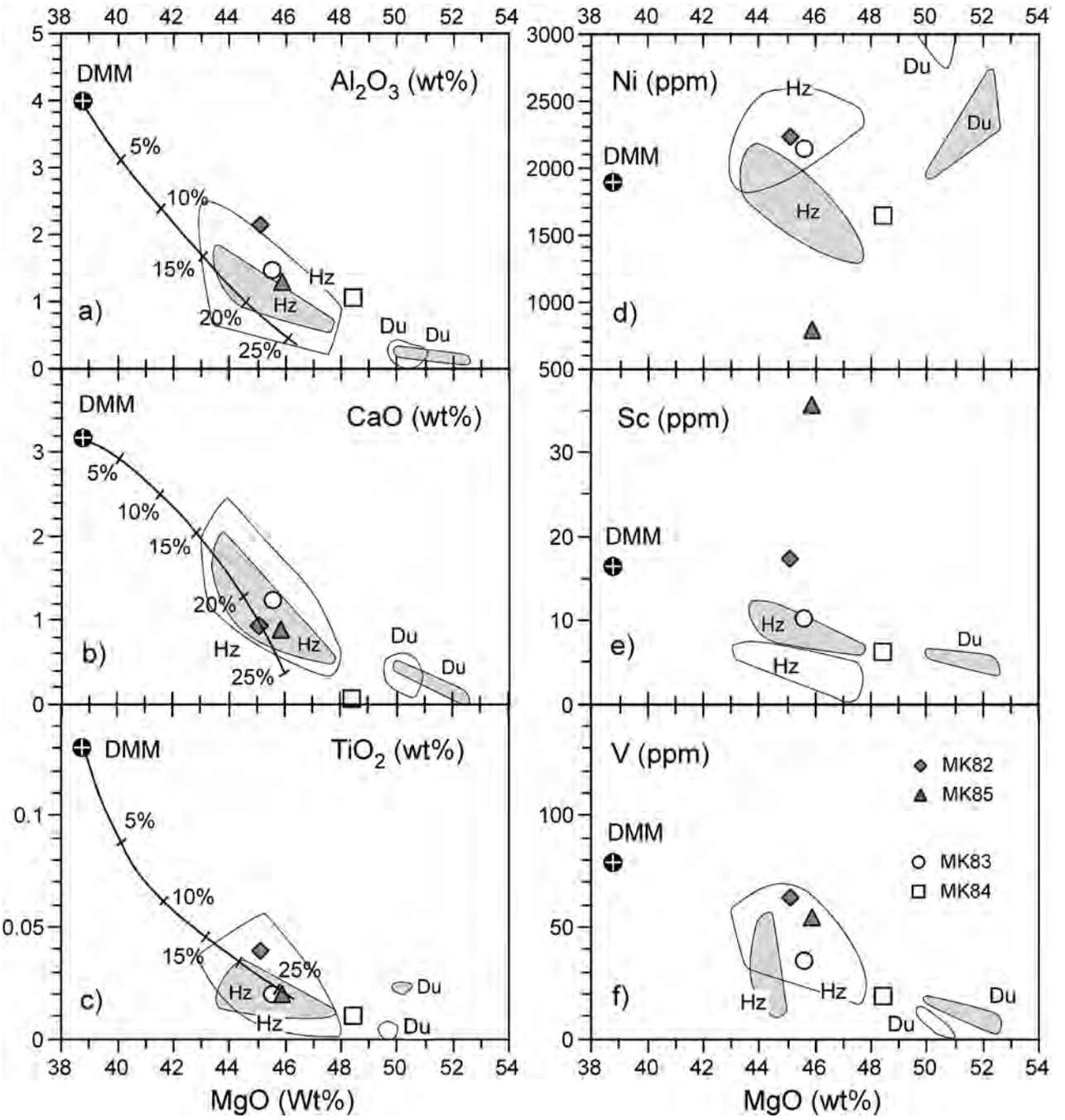

Fig. 12 - Variation of selected major and trace elements vs. MgO for the Sorkhband peridotites. Major element concentrations are recalculated to 100% on LOI-free and secondary calcite-free bases. Shaded fields represent the compositional variation of harzburgites (Hz) and dunites (Du) from the Sorkhband ultramafic complex (Najafzadeh et al., 2008). Open fields encompass the compositions of harzburgites and dunites from the Haji-Abad ophiolites (Shafaii Moghadam et al., 2013), Kermanshah ophiolite (Allahyari et al., 2010), and Nehbandan ophiolite (Saccani et al., 2010). Partial melting trend shows residual spinel peridotite major element compositions during anhydrous polybaric near-fractional melting of the depleted MORB mantle (DMM) source (Workman and Hart, 2005) calculated using the model of Niu (1997). Numbers along the lines indicate percent melting.

components (see Saccani et al., 2015). The second stage is associated with oceanic consumption in a nascent forearc setting (e.g., Saccani et al., 2010; 2013; Shafaii Moghadam et al., 2013; Allahyari et al., 2014).

Due to the lack of E-MORB type gabbros, as well as of volcanic rocks in the Sorkhband upper tectonic slice, a straightforward correlation between these ophiolites and other ophiolitic complexes in Iran cannot be made. Nonetheless, though the data set is limited, the N-MORB chemistry of gabbros from the upper tectonic slice of the Sorkhband ophiolite suggests that these rocks record a stage of oceanic spreading.

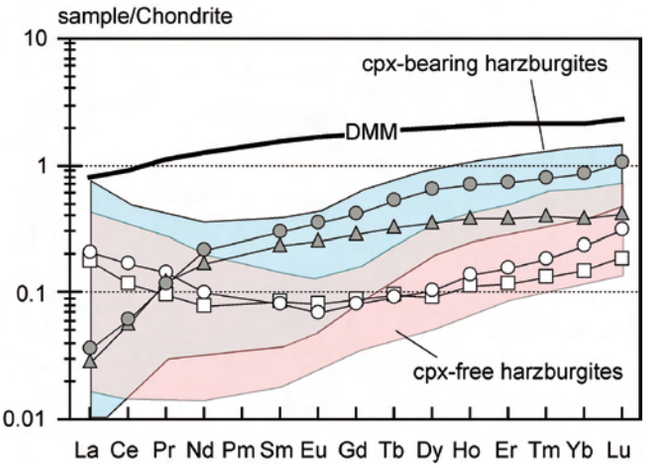

Fig. 13 - Chondrite-normalized REE patterns for the Sorkhband peridotites. Normalizing values are from Sun and McDonough (1989). The compositional variations (gray fields) of clinopyroxene (cpx)-bearing harzburgites and cpx-free harzburgites from Haji-Abad ophiolites (Shafaii Moghadam et al., 2013), Kermanshah ophiolite (Allahyari et al., 2010), and Nehbandan ophiolite (Saccani et al., 2010) are also shown for comparison.

As described above, mantle peridotites from the lower tectonic slice show variably depleted features. Apart from those elements that were likely mobilized during seafloor alteration, both major and trace elements are in the compositional range for Mesozoic harzburgites from various ophiolitic complexes of Iran that were generated at SSZ (Ghazi and Hassanipak, 1999; Delavari et al., 2009; Saccani et al., 2010; Allahyari et al., 2010; Shafaii Moghadam and Stern, 2011; Shafaii Moghadam et al., 2013; Saccani et al., 2013), as well as from the Sorkhband ultramafic complex (Najafzadeh et al., 2008) (Fig. 12). Accordingly, when compared to the SSZ harzburgites from different Iranian ophiolitic complexes, samples MK82 and MK85 have REE patterns similar to those of clinopyroxene-bearing harzburgites, whereas samples MK83 and MK84 have REE patterns similar to those of clinopyroxene-free depleted harzburgites (Fig. 13). Partial melting curves calculated for major elements starting from the DMM source (Workman and Hart, 2005) according to the model of Niu (1997) are shown in Fig. 12a-c. Taking into account the possible effect of seafloor alteration, as described above (i.e., Al_2O_3 gain in samples MK 82 and MK84 and CaO loss in sample MK84), the major element composition of the studied peridotites is generally compatible with the compositions of mantle residua after high degrees of partial melting (> 20%) of a DMM source. Such high degrees of partial melting are commonly observed in depleted lherzolites and harzburgites from SSZ settings, where they are the result of multi-stage mantle melting (see Shervais, 2001; Saccani et al., 2011). However, the LREE enrichment relative to MREE observed in the depleted harzburgites MK83 and MK84 cannot be simply explained as a result of partial melting of primitive mantle. Such an LREE/MREE enrichment can be explained basically by: 1) hydrothermal alteration and serpentinization (e.g., Paulick et al., 2006; Delacour et al., 2008); 2) metasomatism by slab-derived fluids (e.g., Parkinson and Pearce, 1998). However, hydrothermal alteration and serpentinization will result in LREE/MREE ratios totally unrelated to the absolute Yb content. In contrast, in the studied rocks, the $(La/Sm)_N$ ratios show a negative correlation with Yb_N values (not shown). In other words, the $(La/Sm)_N$ ratios increase as the Yb_N values decrease (i.e., the depletion degree increase). This allows us to exclude that the LREE/MREE enrichment observed in depleted harzburgites MK83 and MK84 is associated with hydrothermal alteration and serpentinization. Therefore, such LREE/MREE enrichment can be explained by mantle metasomatism by slab-derived fluids in SSZ setting following an earlier depletion event. The REE composition of depleted harzburgites is compatible with the composition of mantle residua after boninitic melt extraction (e.g., Saccani et al., 2011). Accordingly, several authors (Najafzadeh et al., 2008; Behzadi and Shahabpour, 2011; Jannessary et al., 2012; Najafzadeh, 2012; Rajabzadeh and Moosavinasab, 2013) have shown that the composition of chromian-spinel in chromitite ore bodies from the Sorkhband ultramafic complex is compatible with an origin from a boninitic melt under a low oxygen fugacity in a SSZ setting.

Our new data indicate that the shear zone between the Coloured Mélange and the Bajgan Complexes bears slices of ophiolites derived from two different oceanic domains representing two different geodynamic settings. This occurrence provides new evidence that the boundary between the Coloured Mélange and the Bajgan Complexes represents a first-order tectonic structure that played an important role in the geodynamic evolution of the Makran area. Unfortunately, very few data on the geology of the area studied in this paper are available. In consequence, the new data presented herein highlight the importance of improving the geological and tectonic knowledge on this area in order to better define the significance of this main tectonic structure within the framework of the geodynamic evolution of the Makran.

CONCLUSIONS

In the North Makran, a major shear zone marks the boundary between the Coloured Mélange and the Bajgan-Durkan Complexes. This shear zone consists of deformed rocks extending for ~ 500 km along the whole Makran area. This shear zone is characterized by slices of ophiolites cropping out in the Sorkhband and Rudan areas. Preliminary geological and petrological studies of these ophiolites from the Sorkhband area are presented in this paper. Results of these studies can be summarized as follows.

1) Ophiolites in the Sorkhband area are represented by two different tectonic slices. The upper tectonic slice consists of gabbros, whereas the lower tectonic slice consists of mantle peridotites associated with dunites and chromitite ore deposits.

2) Petrography and geochemistry of the gabbros clearly indicate an N-MORB type affinity suggesting that they were generated at mid-ocean ridge setting. Their chondrite-normalized REE patterns indeed show the typical N-MORB trend with flat medium MREE-HREE coupled with LREE depletion (La_N/Yb_N = 0.44-0.62). Consistent with the petrographic analyses, they display Eu positive anomalies indicating early crystallization of plagioclase.

3) Mantle peridotites consist of harzburgites and depleted harzburgites, both showing marked depletion in incompatible elements and REE. Harzburgites are characterized by severe depletion in LREE compared to MREE and HREE. In contrast, depleted harzburgites show comparatively lower absolute concentrations of HREE and LREE/MREE enrichment (i.e., U-shaped REE patterns). Both major element and REE compositions are compatible with the compositions of mantle residua after high degrees

(> 20%) of partial melting of a depleted mantle source. The REE composition of depleted harzburgites is compatible with the composition of mantle residua after boninitic melt extraction. Moreover, the LREE/MREE enrichment observed in the depleted harzburgites can be explained by mantle metasomatism by slab-derived fluids in SSZ setting following an earlier depletion event. All these features point out for a genesis in a SSZ setting.

4) The new data presented in this paper indicate that the shear zone between the Coloured Mélange and the Bajgan Complexes bears slices of ophiolites derived from two different oceanic domains representing two different geodynamic settings. This occurrence provides new evidence that the boundary between the Coloured Mélange and the Bajgan Complex represents a first-order tectonic structure that played an important role in the geodynamic evolution of the Makran area.

ACKNOLEDGEMENTS

The research has been funded by Darius Project (resp. M. Marroni). This research benefits also by grants from PRA project of University of Pisa (resp. S. Rocchi) and from IGG-CNR. Mr. Sayyareh from Geological Survey of Iran is thanked for helping with field works. R. Tassinari and M. Bonora (University of Ferrara) are acknowledged for their technical support with chemical analyses and thin sections, respectively. We are grateful to K. Sayit and A. Photiades for their constructive reviews of this paper, as well as to the Editor A. Montanini for her helpful comments.

REFERENCES

Allahyari K., Saccani E., Pourmoafi M., Beccaluva L. and Masoudi F., 2010. Petrology of mantle peridotites and intrusive mafic rocks from the Kermanshah ophiolitic complex (Zagros belt, Iran): Implications for the geodynamic evolution of the Neo-Tethyan oceanic branch between Arabia and Iran. Ofioliti 35 (2): 71-90.

Allahyari K., Saccani E., Rahimzadeh B. and Zeda O., 2014. Mineral chemistry and petrology of highly magnesian ultramafic cumulates from the Sarve-Abad (Sawlava) ophiolites (Kurdistan, NW Iran): New evidence for boninitic magmatism in intra-oceanic fore-arc setting in the Neo-Tethys between Arabia and Iran. J. Asian Earth Sci., 79: 312-328.

Bayer R., Chery J., Tatar M., Vernant P., Abbassi M., Masson F., Nilforoushan F., Doerflinger E., Regard V. and Bellier O., 2006. Active deformation in Zagros-Makran transition zone inferred from GPS measurements. Geophys. J. Int., 165 (1): 373-381.

Behzadi K.H. and Shahabpour J., 2011. An emplacement model for Esfandagheh and Faryab ultramafic-mafic complexes, Kerman province, south east Iran. N. Jahrb. Geol. Pal. Abh., 262: 25-42.

Burg J-P., Bernoulli D., Smit J., Dolati A. and Bahroudi A., 2008. A giant catastrophic mud-and-debris flow in the Miocene Makran. Terra Nova, 20 (3):188-193.

Burg J-P., Dolati A., Bernoulli D. and Smit J., 2013. Structural style of the Makran Tertiary accretionary complex in SE Iran. In: Al Hosani et al. (Eds.), Frontiers Earth Sci., 5: 239-259.

Delacour A., Früh-Green G.L., Frank M., Gutjahr M. and Kelley D.S., 2008. Sr- and Nd-isotope geochemistry of the Atlantis Massif (30°N, MAR): implication for fluid fluxes and lithospheric heteroneity. Chem. Geol., 254:19-35.

Delavari M., Amini S.A., Saccani E. and Beccaluva L., 2009. Geochemistry and petrogenesis of mantle peridotites from the Nehbandan Ophiolitic Complex, Eastern Iran. J. Appl. Sci. Res., 9: 2671-2687.

Dercourt J., Zonenshian L.P., Ricou L.E., Kazmin V.G., LePichon X., Knipper A.L., Grandjacquet C., Sbortshikov M., Geyssant J., Lepvrier C., Pechersky D. H., Boulin J., Sibuet J.C., Savostin L.A., Sorokhtin O., Westphal M., Bazhenov M.L., Lauer J.P. and Biju-Duval B., 1986. Geological evolution of the Tethys Belt from the Atlantic to the Pamirs since the Lias. Tectonophysics, 123: 241-315.

Desmons J. and Beccaluva L., 1983. Mid-oceanic ridge and island arc affinities in ophiolites from Iran: paleogeographic implication. Chem. Geol., 39: 39-63.

Dolati A. and Burg J-P., 2013. Preliminary fault analysis and paleostress evolution in the Makran Fold-and-Thrust Belt in Iran. In: Al Hosani et al. (Eds.), Frontiers Earth Sci., 5: 261-277.

Gansser A., 1955. New aspects of the geology in central Iran. Paper presented at 4th World Petroleum Congress, Roma, p. 279-300.

Gansser A., 1959. Ausseralpine ophiolithprobleme. Ecl. Geol. Helv., 52 (2): 659-680.

Ghazi A.M. and Hassanipak A.A., 1999. Geochemistry of subalkaline and alkaline extrusives from the Kermanshah ophiolite, Zagros Suture Zone, Western Iran: implications for Tethyan plate tectonics. J. Asian Earth Sci., 17: 319-332.

Ghazi J.M. and Moazzen M., 2015. Geodynamic evolution of the Sanandaj-Sirjan Zone, Zagros Orogen, Iran. Turkish J. Earth Sci., 24: 513-528

Ghazi A.M., Hassanipak A.A., Mahoney J.J. and Duncon R.A., 2004. Geochemical characteristics, ^{40}Ar-^{39}Ar ages and original tectonic setting of the Band-e-Zeyarat/Dar Anar ophiolite, Makran accretionary Prism, S.E. Iran. Tectonophysics, 193: 175-196.

Glennie K.W., 2000. Cretaceous tectonic evolution of Arabia's Eastern plate margin: a tale of two oceans. SEPM Spec. Publ., 69: 9-20.

Govindaraju K., 1994. Geostand. Newsl., Spec. Issue, 118: 158 pp.

Grando G. and McClay K., 2007. Morphotectonics domains and structural styles in the Makran accretionary prism, offshore Iran. Sedim. Geol., 196: 157-179.

Hart S.R. and Zindler A., 1986. In search of the bulk Earth composition. Chem. Geol., 57: 247-267.

Hunziker D., Burg J-P., Bouilhol P. and von Quadt A., 2015. Jurassic rifting at the Eurasian Tethys margin: Geochemical and geochronological constraints from granitoids of North Makran, southeastern Iran. Tectonics, 34: 571-593.

Jackson M.L., 1958. Soil chemical analysis, Prentice-Hall, New York, 498 pp.

Jagoutz E., Palme H., Baddenhausen H., Blum K., Candales M., Dreibus C., Spettel B., Lorenz V. and Wanke H., 1979. The abundances of major and trace elements in the earth's mantle as derived from primitive ultramafic nodules. Proc. Lunar Planet. Sci., Conf., 10: 2031-2050.

Jannessary M.R., Melcher F., Lodziak J. and Meisel T.C., 2012. Review of platinum-group element distribution and mineralogy in chromitite ores from southern Iran. Ore Geol. Rev., 48: 278-305.

Lachance G.R. and Trail R.J., 1966. Practical solution to the matrix problem in X-ray analysis. Can. Spectrosc., 11: 43-48.

Masson F., Anvari M., Djamour Y., Walpersdorf A., Tavakoli F., Daignières M., Nankali H. and Van Gorp S., 2007. Large-scale velocity field and strain tensor in Iran inferred from GPS measurements: new insight for the present-day deformation pattern within NE Iran. Geophys. J. Int., 170: 436-440.

McCall G.J.H., 1983. Mélanges of the Makran, southeastern Iran. In: G.J.H. McCall (Ed.), Ophiolitic and related mélanges. Hutchinson Ross Publ. Comp., Stroudsburg, Pennsylvania. Benchmark Papers in Geol., 66: 292-299

McCall G.J.H., 1985. Explanatory text of the Minab Quadrangle Map; 1:250,000, No. J13. Geol. Surv. Iran, Tehran, 530 pp.

McCall G.J.H., 1997. The geotectonic history of the Makran and adjacent areas of southern Iran. J. Asian Earth Sci. 15 (6): 517-531.

McCall G.J.H., 2002. A summary of the geology of the Iranian Makran. In: P.D. Clift, F.D. Kroon, C. Gaedecke and J. Craig (Eds.), The tectonic and climatic evolution of the Arabian Sea Region. Geol. Soc. London Spec. Publ., 195: 147-204.

McCall G.J.H. and Kidd R.G.W., 1982. The Makran southeastern Iran: the anatomy of a convergent margin active from Cretaceous to present. In: J.K. Leggett (Ed.), Trench-forearc geology: sedimentation and tectonics of modern and ancient plate margins. 10: 387-397.

McQuarrie N., Stock J.M., Verdel C. and Wernicke B.P., 2003. Cenozoic evolution of Neotethys and implications for the causes of plate motions. Geophys. Res. Lett., 30: 2036. doi: 10.1029/2003GL017992.

Morgan K.H, McCall G.J.H. and Huber H., 1979. Minab Quadrangle Map 1:250,000. Ministry of Mines and Metal., Geol. Surv. Iran.

Moslempour M.E., Khalatbari-Jafari M., Ghaderi M., Yousefi H. and Shahdadi S., 2015. Petrology, geochemistry and tectonics of the extrusive sequence of Fanuj-Maskutan Ophiolite, Southeastern Iran. J. Geol. Soc. India, 85: 604-618.

Najafzadeh A., 2012. The geochemistry of the whole rock and Platinum-group elements in pyroxenites of Sorkhband Ultramafic Complex, Southern Iran. Int. Conf. Geol. Environ. Sci., IPCBEE, Singapoore, 36: 11-15

Najafzadeh A.R., Arvin M., Pan Y. and Ahmadipour H., 2008. Podiform chromitites in the Sorkhband Ultramafic Complex, Southern Iran: Evidence for ophiolitic chromitite. J. Sci., Islamic Republic Iran, 19: 49-65.

Niu Y., 1997. Mantle melting and melt extraction processes beneath ocean ridges: evidence from abyssal peridotites. J. Petrol., 38: 1047-1074.

Parkinson I.J. and Pearce J.A., 1998. Peridotites from the Izu-Bonin-Mariana forarc (ODP Leg 125): evidence for mantle melting and melt-mantle interaction in a suprasubduction zone setting. J. Petrol., 39: 1577-1618.

Paulick H., Bach W., Godard M., De Hoog J.C.M., Suhr G. and Harvey J., 2006. Geochemistry of abyssal peridotites (mid-Atlantic Ridge, 158200 N, ODP Leg 209): Implications for fluid/rock interaction in slow spreading environments. Chem. Geol., 234: 179-210.

Rajabzadeh M.A. and Moosavinasab Z., 2013. Mineralogy and distribution of Platinum-Group Minerals (PGM) and other solid inclusions in the Faryab ophiolitic chromitites, Southern Iran. Mineral. Petrol.,107: 943-962

Saccani E., 2015. A new method of discriminating different types of post-Archean ophiolitic basalts and their tectonic significance using Th-Nb and Ce-Dy-Yb systematics. Geosci. Frontiers, 6: 481-501.

Saccani E., Allahyari K., Beccaluva L. and Bianchini G., 2013. Geochemistry and petrology of the Kermanshah ophiolites (Iran): Implication for the interaction between passive rifting, oceanic accretion, and plume-components in the Southern Neo-Tethys Ocean. Gondwana Res., 24: 392-411.

Saccani E., Beccaluva L., Photiades A. and Zeda O., 2011. Petrogenesis and tectono-magmatic significance of basalts and mantle peridotites from the Albanian-Greek ophiolites and sub-ophiolitic mélanges. New constraints for the Triassic-Jurassic evolution of the Neo-Tethys in the Dinaride sector. Lithos, 124: 227-242.

Saccani E., Delavari M., Beccaluva L. and Amini S.A., 2010. Petrological and geochemical constraints on the origin of the Nehbandan ophiolitic complex (eastern Iran): Implication for the evolution of the Sistan Ocean. Lithos 117: 209-228.

Saccani E., Dilek Y., Marroni M. and Pandolfi L., 2015. Continental margin ophiolites of Neotethys: Remnants of ancient ocean-continent transition Zone (OCTZ) lithosphere and their geochemistry, mantle sources and melt evolution patterns. Episodes, 38: 230-249.

Serri G., 1981. The petrochemistry of ophiolite gabbroic complexes: a key for the classification of ophiolites into low-Ti and high-Ti types. Earth Planet. Sci. Lett., 52: 203-212.

Shafaii Moghadam H. and Stern R.J., 2011. Geodynamic evolution of Upper Cretaceous Zagros ophiolites: formation of oceanic lithosphere above a nascent subduction zone. Geol. Mag., 148: 762-801.

Shafaii Moghadam H., Stern R. J., Chiaradia M. and Rahgoshay M., 2013. Geochemistry and tectonic evolution of the Late Cretaceous Gogher-Baft ophiolite, central Iran. Lithos, 168-169: 33-47.

Shaker-Ardakani A.R., Arvin M., Oberhänsli R., Mocek B. and Moeinzadeh S.H., 2009. Morphology and petrogenesis of pillow lavas from the Ganj Ophiolitic Complex, Southeastern Kerman, Iran. J. Sci., Islamic Republic Iran, 20 (2): 139-151.

Shervais J.W., 2001. Birth, death, and resurrection: The life cycle of suprasubduction zone ophiolites. G3- Geochem. Geophys. Geosyst., 2: 1-45.

Snow J.E. and Dick H.J.B., 1995. Pervasive magnesium loss by marine weathering of peridotite. Geochim. Cosmochim. Acta, 59: 4219-4235.

Sun S.S. and McDonough W.F., 1989. Chemical and isotopic-systematics of oceanic basalts: implications for mantle composizion and processes. In: A.D. Saunders and M.J. Norry (Eds.), Magmatism in ocean basins. Geol. Soc. London Spec. Publ., 42: 313-345.

Vigny C., Huchon P., Ruegg J., Khanbari K. and Asfaw L.M., 2006. Confirmation of Arabia plate slow motion by new GPS data in Yemen. J. Geophys. Res., 111: B02402, doi: 10.1029/2004JB003229.

Whitechurch H., Omrani J., Agard P., Humbert F., Montigny R. and Jolivet L., 2013. Evidence for Paleocene-Eocene evolution of the foot of the Eurasian margin (Kermanshah ophiolite, SW Iran) from back-arc to arc: Implications for regional geodynamics and obduction. Lithos, 182-183: 11-32.

Wood D.A., 1980. The application of a Th-Hf-Ta diagram to problems of tectonomagmatic classification and to establishing the nature of crustal contamination of basaltic lavas of the British Tertiary volcanic province. Earth Planet. Sci Lett., 50: 11-30.

Workman R.K. and Hart S.R., 2005. Major and trace element composition of the depleted MORB mantle (DMM). Earth Planet. Sci Lett., 231: 53-72.

Received, March 4, 2016
Accepted, May 22, 2016